LEVEE EROSION BY OVERTOPPING DURING THE KATRINA HURRICANE

Jean-Louis Briaud[1] and Hamn Ching Chen[1]
Invited Lecture at the Third International Conference on Scour and Erosion
Amsterdam, November 1-3, 2006

Briaud J.-L., Chen H.-C., 2006, "Levee Erosion by Overtopping During the Katrina Hurricane" Proceedings of the Third International Conference on Scour and Erosion, Amsterdam Nov 1-3, 2006, The Netherlands.

ABSTRACT

Erodibility of a soil is defined here as the relationship between the erosion rate of a soil dz/dt and the velocity v of the water flowing over it or better, the relationship between the erosion rate of a soil dz/dt and the shear stress developed by the water at the water-soil interface. This is called the erosion function. The test used to measure the erosion function of the levee soils is the Erosion Function Apparatus EFA test. The test consist of eroding a soil sample by pushing it out of a thin wall steel tube and recording the erosion rate for a given velocity of the water flowing over it. Several velocities are used and the erosion function is defined. A new erosion category chart is proposed to reduce the erodibility of a soil or rock to a single category number.

The Netherlands is a country with well advanced knowledge on the topic of levee erosion by overtopping. A short review of that knowledge is conducted, including the 1953 levee failures.

Twenty three samples were retrieved from eleven locations at the top of the levees around New Orleans. Thirteen were samples from Shelby tubes while ten were bag samples. The results obtained show a large variation of erosion resistance among the soils tested. Some of the levees associated with the location of the samples resisted the overtopping erosion very well; others eroded completely. This allowed us to prepare a chart which can be used to select soils for overtopping resistance.

Numerical simulations were performed using the program CHEN 3D to obtain the distribution of velocity vectors in the overtopping flow and of shear stresses at the interface between the water and the levee surface. The comparison of the numerical simulations results and of the erosion functions gives added credibility to the proposed levee overtopping erosion chart.

[1] Zachry Department of Civil Engineering, Texas A&M University, College Station, Texas 77843-3136, USA (briaud@tamu.edu)

INTRODUCTION

Hurricane Katrina devastated the New Orleans area on August 29, 2005. Some of the reported numbers include 1300 deaths, 500,000 people having left the area, and some 100 Billion dollars of economic loss. The impact of that storm was significantly increased by the fact

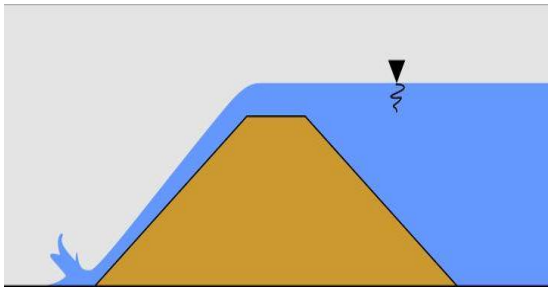

Figure 1 – Levee overtopping.

that some levees failed. There seems to be two major and very different

mechanisms associated with the failures:

sliding and erosion. This paper addresses the erosion aspect of the New Orleans levees as they were overtopped (Fig. 1 and 2).

The overtopping process shown in Fig. 1 is investigated by presenting the results of erosion tests on samples collected from the levees, as well as numerical simulations and a review of the knowledge in Netherlands. A comparison is made between the analysis work and the observations during the hurricane. This process helps in proposing an erosion resistance chart in the case of levee overtopping.

ERODIBILITY: A DEFINITION

Erodibility is a term often used in scour and erosion studies. Erodibility may be thought of as one number which characterizes the rate at which a soil is eroded by the flowing water. With this concept erosion resistant soils would have a low erodibility number and erosion sensitive soils would have a high erodibility number. This concept is not appropriate; indeed the water velocity can vary drastically from say 0 m/s to 5 m/s or more and therefore erodibility is a not a single number but a relationship between the velocity applied and the corresponding erosion rate experienced by the soils (Fig. 3, 4). While this is an improved definition of erodibility, it still presents some problems because water velocity is a vector quantity which varies everywhere in the flow and is theoretically zero at the soil water interface. It is preferable to quantify the action of the water on the soil by using the shear stress applied by the water on the soil at the water-soil interface. Erodibility is therefore defined here as the relationship between the erosion rate

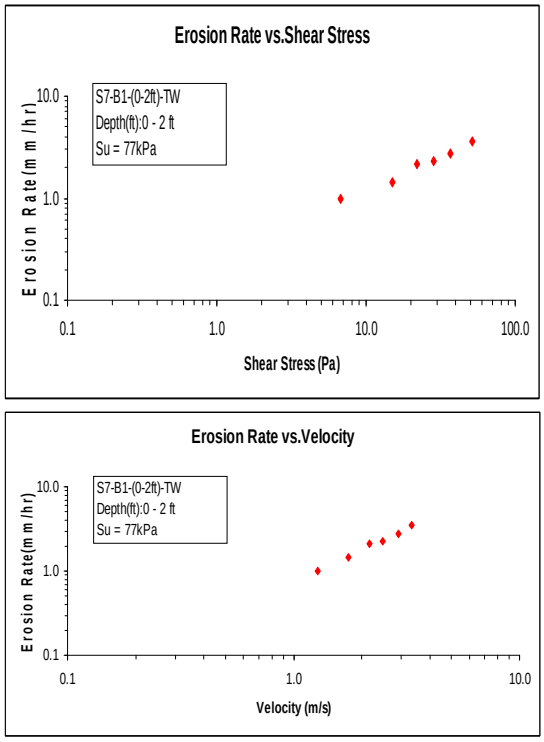

Figure 3 Erodibility function for a clay: EFA Test Results for Sample No. S7-B1-(0-0.6 m)-TW, Sample Type: Shelby Tube, Water Salinity: 0.4 PPT (Tap Water).

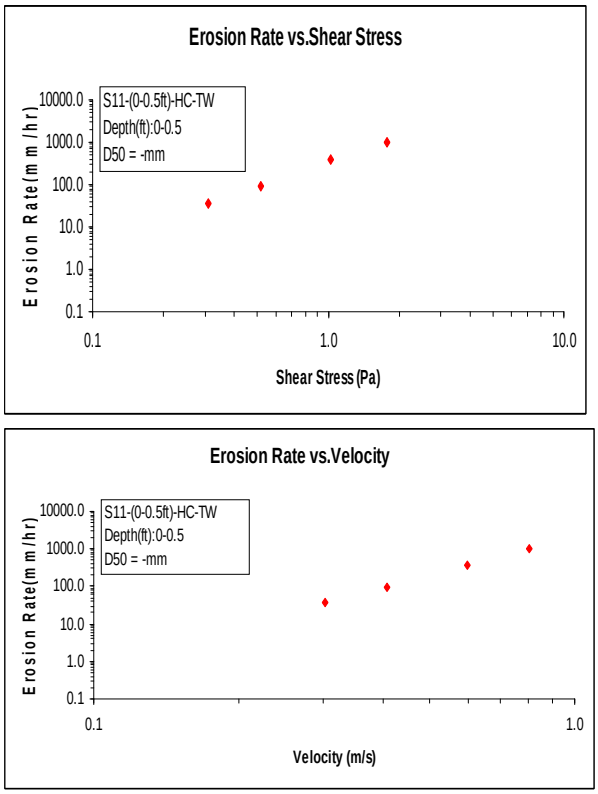

Figure 4 Erodibility function for a clay: EFA Test Results for Sample No. S11-(0-0.15 m)-HC-TW, Sample Type: Bulk Sample, Water Salinity: 0.4 PPT (Tap Water), Compaction Effort: High = 100% Modified Proctor Compaction

$\dot{z}$ and the hydraulic shear stress applied τ (Fig. 3, 4). This relationship is called the erosion function $\dot{z}(\tau)$. The erodibility of a soil or a rock is represented by the erosion function of that soil or rock. This erosion function can be obtained by using a laboratory device called the EFA (Erosion Function Apparatus, Briaud et al., 2001a) and described later.

The idea of quantifying the erodibility of a soil or rock by a single number is attractive because of its simplicity. In order to retain the advantage of that simplicity while not having the drawback discussed above, erosion categories are proposed (Fig. 5). An erodibility category of I corresponds to a

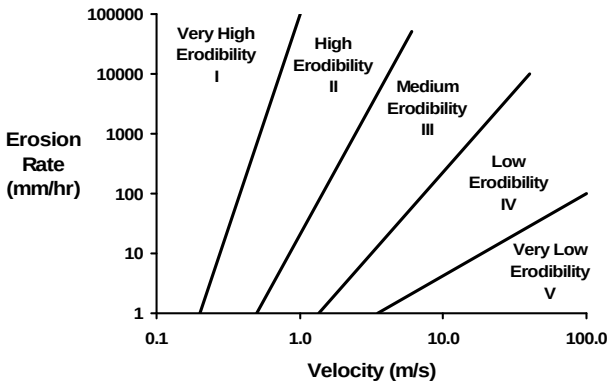

Figure 5 Erosion Categories.

range of erodibility functions falling in the area marked I on Fig. 5. Note first that, contrary to the comment made earlier, velocities are used instead of shear stresses. This is done for the sake of simplicity and as a first step in establishing the categories. Indeed one tends to have much more feel for the magnitude of water velocities than for the magnitude of hydraulic shear stresses. In the long term it is planned to propose a more theoretically satisfying

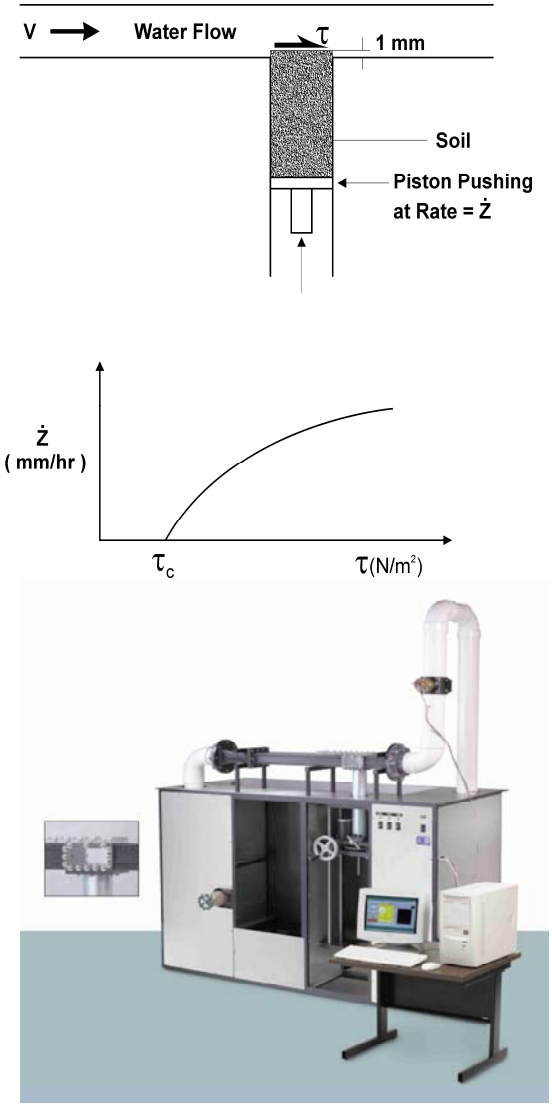

Figure 6 EFA (Erosion Function Apparatus) from Briaud et al. (2001)

set of erosion categories. Note also that erodibility takes the form of a single number when it comes to the erosion threshold (critical velocity or critical shear stress) exhibited by soils and rocks. The range of critical velocities associated with the proposed categories can be read on the horizontal axis of the erodibility chart (Fig. 5).

THE EFA: EROSION FUNCTION APPARATUS

The EFA (Briaud et al. 1999, Briaud et al., 2001a) was conceived by Dr. Briaud in 1991, designed in 1992, and built in 1993 (Fig. 6). The original purpose was to develop a method to predict the scour depth at bridge supports (Briaud et al., 2004). The sample of soil, fine-grained or not, is taken in the field by pushing an ASTM standard Shelby tube with a 76.2 mm outside diameter(ASTMD1587). 50.8 mm. The pipe is 1.22 m long and has a flow straightener at one end. The water is driven through the pipe by a pump. A valve regulates the flow and a flow meter is used to measure the flow rate. The range of mean flow velocities is 0.1 m/s to 6 m/s. The end of the Shelby tube is held flush with the bottom of the rectangular pipe. A piston at the bottom end of the sampling tube pushes the soil until it protrudes 1 mm into the rectangular pipe at the other end. This 1 mm protrusion of soil is eroded by the water flowing over it.

EFA test procedure

The procedure for the EFA test consists of

1. Place the sample in the EFA, fill the pipe with water, and wait one hour.
2. Set the velocity to 0.3 m/s.
3. Push the soil 1 mm into the flow.

4. Record how much time it takes for the 1 mm soil to erode.
5. When the 1 mm of soil is eroded or after 30 minutes of flow whichever comes first, increase the velocity to 0.6 m/s and bring the soil back to a 1 mm protrusion.
6. Repeat step 4.
7. Then repeat steps 5 and 6 for velocities equal to 1.0 m/s, 1.5 m/s, 2 m/s, 3 m/s, 4.5 m/s, and 6 m/s. The choice of velocity can be adjusted as needed.

EFA test data reduction

The test result consists of the erosion rate dz/dt versus shear stress τ curve (Fig. 3, 4, and 6). For each flow velocity v, the erosion rate dz/dt (mm/hr) is simply obtained by dividing the length of sample eroded by the time required to do so.

$$dz/dt = h/t \qquad (1)$$

where h is the length of soil sample eroded in a time t. The shear stress τ is obtain by using the Moody Chart (Moody, 1944) for pipe flows.

$$\tau = f \rho v^2/8 \qquad (2)$$

Where τ is the shear stress on the wall of the pipe, f is the friction factor obtained from Moody Chart (Fig. 7), ρ is the mass density of water (1000 kg/m3), and v is the mean flow velocity in the pipe. The friction factor f is a function of the pipe Reynolds number Re and the pipe roughness ε/D. The Reynolds number is $Re = vD/\nu$ where D is the pipe diameter and ν is the kinematic viscocity of water (10^{-6} m^2/s at 20^0C). Since the pipe in the EFA has a rectangular cross section, D is taken as the hydraulic diameter D = 4A/P (Munson et al., 1990) where A is the cross sectional flow area, P is the wetted perimeter, and the factor 4 is used to ensure that the hydraulic diameter is equal to the diameter for a circular pipe. For a rectangular cross section pipe:

$$D = 2ab/(a + b) \qquad (3)$$

where a and b are the dimensions of the sides of the rectangle. The relative roughness ε/D is the ratio of the average height of the roughness elements on the pipe surface over the pipe diameter D. The average height of the roughness elements ε is taken equal to $0.5D_{50}$ where D_{50} is the mean grain size for the soil. The factor 0.5 is used because it is assumed that the top half of the particle protrudes into the flow while the bottom half is buried into the soil mass. During the test, it is possible for the soil surface to become rougher than 0.5 D_{50}; this occurs when the soil erodes block by block rather than particle by particle. In this case the value used for ε is estimated by the operator on the basis of inspection through the test window. Typical EFA test results are shown on Fig. 3 and 4 for a low and high erodibility soil.

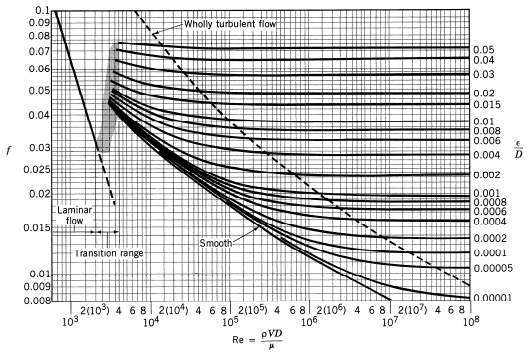

Figure 7 Moody Chart (reprinted with permission from Munson et al. 1990)

PRACTICE IN THE NETHERLANDS

1953 Levee (Dike) failures in Netherlands (Gerritsen, 2006)

The Netherlands is a country of 16 Million people and 26% of them live below mean sea level protected by seadikes, dunes and levees. For centuries, the federal government and local water boards are responsible for dike design and maintenance. Prior to 1953 the dikes were at a height equal to the maximum recorded water level plus 0.5 m. The height of some of the levees had been increased by constructing concrete walls along the levee crest. During World War II, the levees were used as a defense system and many holes were dug to that effect. After the war, the damage done to the levees was not adequately repaired.

On January 31, 1953, a North Sea storm combined with high tide and raised the water level to unprecedented height and 150 levee breaches occurred. During that storm, 1836 people died, 100,000 people evacuated, tens of thousands of livestock perished, and 136,500 hectares were inundated. The levee breaches were attributed to sustained wave overtopping. The land side of the levees was typically at a steeper slope (1v to 1.5h or 1v to 2h) than the sea side (1v to 3h or steeper). The failure process initiated from the land side and progressed backward towards the sea side. One sign of imminent failure was a longitudinal crack forming along the crest of the levee which was quickly filled by the rushing water.

On February 18, 1953, a committee was formed called the Delta Committee with the task of ensuring that such a disaster would not happen again. The committee chose to solve the problem not by increasing the height of the levees but rather by recommending the Delta Plan. This plan consisted of closing the shoreline completely through a series of permanent barriers to be built over a 20 year period. In 1975, due to political pressures from the fishing industry and increased environmental awareness, one of the barriers was changed from complete damming to a moveable storm surge barrier to be closed only in the event where a North Sea storm would coincide with a high tide.

The Netherlands now requires that the flood protection systems against attacks from the sea satisfy the following

- Be able to resist a storm surge with a probability of occurrence of 1/10,000 for the Provinces in central Holland.
- Be able to resist a storm surge with a probability of occurrence of 1/4000 for less populated coastal areas.
- Be reviewed and evaluated every 5 years with associated recommendations to be constructed in the following 5 years.

Design consideration for levee erosion in The Netherlands.

The performance of levees impacted by waves and overtopping has been the subject of extensive research in the Netherlands after the disaster of 1953. Many of the collapsed levees in 1953 resulted from inner slope (Fig. 8) shearing following overtopping. To prevent future overtopping, the design of levees has focused on ensuring that the

crown is at an appropriate height (TAW, 1998). This is determined by the level of protection required for the land. For Dutch levees, the ultimate potential threat is chosen from storm surge levels with a 1% per century probability of exceedance (Pilarczyk, 1992). The purpose of the remaining levee elements is to maintain the crown position (Fig. 8).

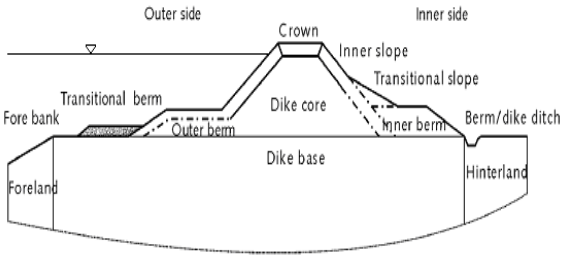

Figure 8 General Profile of Sea Dike (TAW, 1998)

As the soil becomes saturated during overtopping, splits develop parallel to the crown. This allows more water to enter the dike leading to shearing of the inner slope. As the inner slope layer is removed by the water, the core of the levee begins to erode causing the formation of a breach. The growth of the breach is time-dependent and can be predicted by two different approaches: a simple model and an advanced model (Verheij, 2002, Verheij, 2006).

The simple model predicts the breach width (B) as a function of time (t) and soil type (Eqns. 4-5). It is validated by data on breaches from small-scale tests and observations (Fig. 9). The advanced model takes into account the physical behavior of soils as a result of overtopping and infiltration. It provides the velocities at the boundaries of a breach.

$$B = 67 \log\left(\frac{t}{522}\right) \text{ for SAND} \qquad (4)$$

$$B = 20 \log\left(\frac{t}{288}\right) \text{ for CLAY} \qquad (5)$$

Equations 4 and 5 are older equations which have been replaced by the equation in Fig. 9

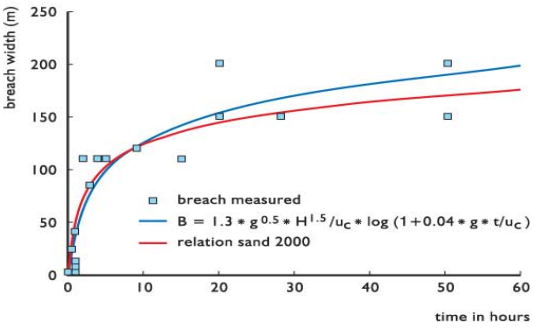

Figure 9 - Breach Width vs. Time (Verheij, 2002, 2006)

Two recommendations exist for the overtopping flow: 0.1 l/m/s (TAW, 1998) or 2 l/m/s (Simm, 2005). Below this threshold, it is not necessary to design for overtopping This assumes that, at that point, saturation of the top slope layer occurs which leads to erosion of the inner slope. The erosion is affected by the soil properties of the slope, the angle of the slope, the amount of overtopping flow, and the quality of the vegetation (TAW, 1998). The most common soil types in the Netherlands are sand, clay, peat, and a mixture of these. There are four categories in which the soil can be described, related to its resistance to erosion (Table 1). Assuming complete saturation, the resistance to erosion can be quickly ascertained by knowing the soil category and the angle of the slope (Fig. 10).

Table 1 Description of Soil Categories (after CROW, 2000)

	SOIL CATEGORY			
	1	2	3	4
Type of Soil	Clay	Clay	Clay	Sand
LL	> 45%	< 45%	< 45%	-
PI	> 18%	> 18%	< 18%	-
% Sand	< 40%	< 40%	> 40%	-
% Lutum	-	-	> 8%	< 8%

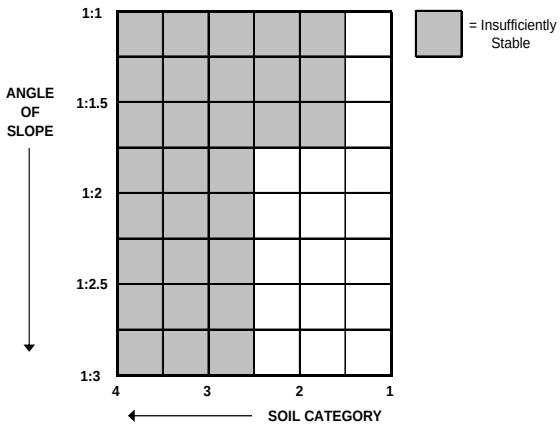

Figure 10 Indication of erosion resistance to overtopping (after TAW, 1998)

When designing a dike, the following requirements must be considered and formulated (Pilarczyk, 1992):

1. The levee should offer the necessary protection against inundation at an acceptable risk.
2. A regional perspective must be taken in order to interpret events at a dike.
3. It must be possible to manage and maintain the structure.
4. Landscape, recreational, and ecological viewpoints should be considered in the design.
5. Construction costs should be minimized at an acceptable risk level. This is typically the controlling factor in the design.
6. Legal restrictions should be identified.

An important design consideration is the placement of a revetment on the levee. Revetments serve as an armor to protect the dike and act as an energy absorber reducing the impact of incoming waves. They can also contribute to water tightness of a dike (TAW, 1998). There are several materials that can be used for a revetment such as grass-cover, rocks, asphalt, and concrete. A grassed clay dike revetment is the most applied type of revetment (Fig. 11). Its primary function is to prevent erosion due to hydraulic forces (Seijffert & Verheij, 1998).

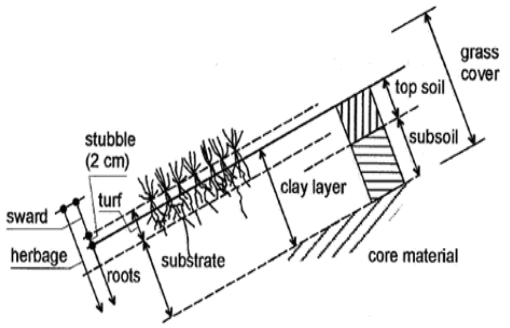

The behavior of the revetments under hydraulic loading depends on the weight, size, and distribution of the revetment material. For grass covers, resistance to erosion is largely due to the 50-150 mm thick dense root system in the top layer of soil or turf (Seijffert, Verheij, 1998).

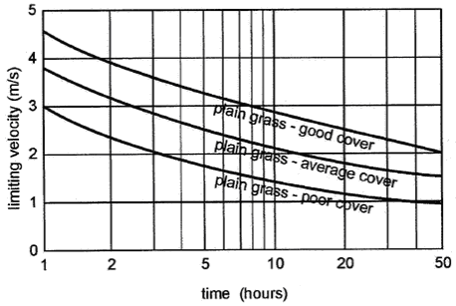

Figure 12 Limiting Velocities for Plain Grass (Seijffert & Verheij, 1998)

The turf cover can resist flow velocities of up to 2 m/s with no problem. Depending on the duration of the flow, higher velocities can be permitted (Fig. 12). Note however that Fig. 12 is for continuous flow and not necessarily for intermittent flow. The standard Dutch practice allows for a design flow of 0.002 m^3/s. For a good quality grass cover, however, recent experience

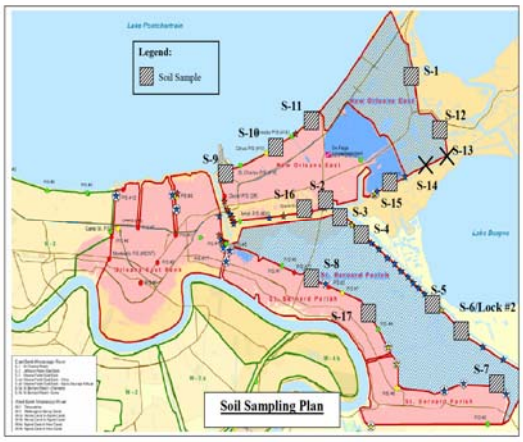

Figure 13 Location of samples

suggests that this flow can be safely increased to 0.005 m^3/s – 0.01 m^3/s. The maximum slope angle for the dike is typically determined by the stability of the revetment. Gentler slopes tend to reduce hydraulic forces on the revetment and provide a greater length over which energy can be dissipated. Mild slopes can also minimize scour at the toe. A common Dutch practice is to apply a slope between 1:3 and 1:5 on the outer slope and 1:3 on the inner slope (Pilarczyk, 1992).

NEW ORLEANS LEVEE SOIL SAMPLES USED FOR EROSION TESTS

A total of 11 locations along the New Orleans levee system were identified for studying the erosion resistance of the levee soils. Emphasis was placed on levees which were very likely overtopped. The samples locations are labeled S1 through S15 for Site 1 through Site 15 on Fig. 13. The samples were taken by pushing a Shelby tube when possible or using a shovel to retrieve soil samples into a plastic bag.

For example at Site S1, the drilling rig was driven on top of the levee, was stopped at the location of Site 1, then a first Shelby tube was pushed with the drilling rig from 0 to 2 ft depth and then a second Shelby tube was pushed from 2 to 4 ft depth in the same hole. These two Shelby tubes belonged to boring B1. The drilling rig advanced a few feet and a second location B2 at Site S1 was chosen; then two more Shelby tubes were collected in the same way as for B1. This process at Site S1 generated 4 Shelby tube samples designated

- S1-B1-(0-2ft)
- S1-B1-(2-4ft)
- S1-B2-(0-2ft)
- S1-B2-(2-4ft)

Four such Shelby tubes were collected from sites S1, S2, S3, S7, S8, and S12. In a number of cases, Shelby tube samples could not be obtained because access for the drilling rig was not possible (e.g.: access by light boat for the Mississippi River Gulf Outlet, MRGO levee) or pushing a Shelby tube did not yield any sample (clean sands). In these cases, grab samples were collected by using a shovel and filling a plastic bag. The number of bags collected varied from 1 to 4. Plastic bag samples were collected from sites S4, S5, S6, S11, and S15. The total number of sites sampled for erosion testing was therefore 11. These 11 sites generated a total of 34 samples. One of the samples, S8-B1-(2-4ft), exhibited two distinct layers during the EFA tests and therefore lead to two EFA curves. All in all 24 EFA curves were obtained from these 34 samples: 14 performed on Shelby tube samples and 10 on bag samples. Some samples were not tested and are stored at Texas A&M University.

EROSION FUNCTION APPARATUS (EFA) TEST RESULTS

Sample preparation

No special sample preparation was necessary for the samples which were in Shelby tubes. The Shelby tube was simply inserted in the hole on the bottom side of the rectangular cross section pipe of the EFA (described previously).

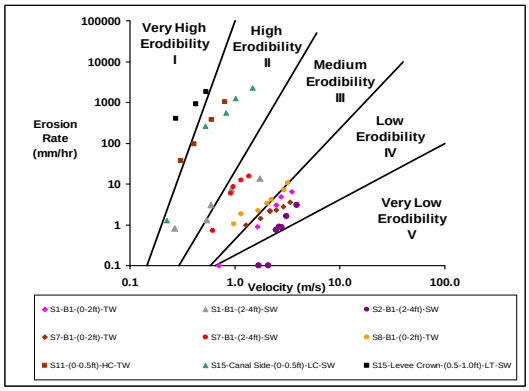

Figure 14 EFA test results for 9 levee samples.

For bag samples obtained by using a shovel to collect the soil, there was a need to reconstruct the sample. These samples were prepared by re-compacting the soil in the Shelby tube. The same process as the one used to prepare a sample for a Proctor compaction test was used. Since it was not known what the compaction level was in the field, two extreme levels of compaction energy were used to re-compact the samples. The goal was to bracket the erosion response of the intact soil. The high compaction effort corresponded to 100% of Modified Proctor compaction effort while the low compaction effort. The low compaction effort corresponded to 1.63% of Modified Proctor compaction effort. More details on the sample preparation of the reconstituted samples can be found in Briaud (2006).

Sample EFA test results

The procedure described earlier was strictly followed for the EFA tests. The results were prepared in the form of a word file report and an accompanying excel spread sheet detailing the data reduction and associated calculations. The main result of an EFA test is a couple of plots: one is the plot of the erosion rate versus mean velocity in the EFA pipe, the other is the plot of the erosion rate versus the calculated shear stress at the interface between the soil and the water. Figs. 3 and 4 show two examples of results for a very erodible soil and a very erosion resistant soil.

Summary erosion chart

In an effort to give a global rendition of the EFA results, an erosion chart was created (Fig. 5). This chart allows one to present the erosion curves by categories. A Category I erosion curve represents a

soil which is very erodible such as clean fine sands. A Category V erosion curve represents a soil which is very erosion resistant such as some high plasticity overconsolidated clays.

Fig. 14 shows the erosion chart populated with the EFA results for all 24 EFA tests. The legend contains the sample/test designation which starts with the site number (Fig. 14), followed by the boring number, the depth, and letter symbols including SW, TW, LC, HC, and LT. SW stands for Sea Water and means that the water used in the EFA test was salt water at a salinity of approximately 35000 ppm. TW stands for Tap Water and means that the water used in the EFA test was Tap Water at a salinity of approximately 500 ppm. LC

stands for Low Compaction, refers to bag samples only, and means that the sample was prepared using 1.6% of Modified Proctor compaction effort. HC stands for High Compaction, refers to bag samples only, and means that the sample was prepared using 100% of Modified Proctor compaction effort. LT stands for Light Tamping and refers to the preparation of some bag samples used in some early tests; it is very similar to the LC preparation.

One of the first observations coming from the summary erosion chart on Fig. 14 is that the erodibility of the soils obtained from the New Orleans levees varies widely all the way from very high erodibility (Category I) to very low erodibility (Category V). This explains in part why some of the overtopped levees failed while other overtopped levees did not. This finding points to the need to evaluate the remaining levees for erodible soils (weak links).

LEVEE OVERTOPPING AND EROSION FAILURE CHART

In an effort to correlate the results of the EFA erosion tests with the behavior of the levees during overtopping flow, Fig. 15 was prepared. It seems reasonably sure that the levees at sites S4, S5, S6, and S15 were overtopped and failed. At the same time it seems reasonably sure that the levees at sites S2, and S3 were overtopped and resisted remarkably well. The dark circles on Fig. 15 correspond to samples taken from levees that were overtopped and failed by erosion while the open circles correspond to samples taken from levees that were overtopped and held during overtopping. Fig. 15 shows a definite correlation between the EFA tests results and the behavior of the levees during overtopping.

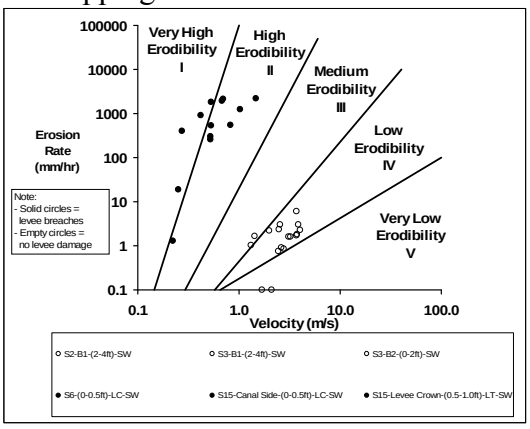

Figure 15 EFA test results and overtopping levee failure/no failure chart

NUMERICAL SIMULATIONS

The program used to perform the numerical simulation was CHEN3D (Computational Hydraulic ENgineering in 3 Dimensions) developed by Chen (2002). In this study, the level-set Reynolds-Averaged Navier-Stokes (RANS) method developed recently by Chen and Yu (2006) was employed for time-domain simulation of levee overtopping under a constant speed current. In this method, the chimera RANS method of Chen and Chen (1998) and Chen (2002) has been employed in conjunction with an interface-capturing method based on the level-set method of Osher and Sethian (1988) for accurate resolution of the air-water interface encountered in levee overtopping simulations. In the present level set formulation, the level set function ϕ is defined as the signed distance from the interface with $\phi < 0$ in air region, $\phi > 0$ in water region, and $\phi = 0$ on the air-water interface. At the beginning of the calculation, the value of ϕ is the physical distance from the interface. It varies smoothly across the interface and is

advected by the local velocity field using the advection equation

$$\frac{\partial \phi}{\partial t} + \vec{V} \cdot \nabla \phi = 0 \tag{6}$$

The interface can be captured at any time by locating the zero level set. In general, the computed ϕ may not remain the signed distance from the interface and needs to be reinitialized for every time step. Sussman et al. (1994) proposed that this be done by solving the following equation until the steady state is reached.

$$\frac{\partial \phi}{\partial \tau} = sign(\phi_0) \cdot (1 - |\nabla \phi|) \tag{7}$$

This guarantees that ϕ has the same sign and zero level as ϕ_0 and satisfies the condition that $|\nabla \phi| = 1$. The evolution of ϕ is given by the advection equation (6) in the transition zone defined by $|\phi| < \varepsilon$, where ε is the half thickness of the interface. In the transition zone, the fluid density and viscosity are smoothed by the Heaviside function $H(\phi)$:

$$\begin{cases} \rho(\phi) = \rho_a + (\rho_w - \rho_a) \cdot H(\phi) \\ \mu(\phi) = \mu_a + (\mu_w - \mu_a) \cdot H(\phi) \end{cases};$$

$$H(\phi) = \begin{cases} 0 & if\ \phi < -\varepsilon \\ \frac{1}{2}\left(1 + \frac{\phi}{\varepsilon} + \frac{1}{\pi}\sin(\frac{\pi\phi}{\varepsilon})\right) & if\ -\varepsilon \le \phi \le \varepsilon \\ 1 & if\ \phi > \varepsilon \end{cases} \tag{8}$$

where the subscripts '*a*' and '*w*' represent air and water, respectively. After a new level set value ϕ_0 is obtained in each time step, it is necessary to solve the re-distancing equation (7) in order to ensure that the level set value remains as a real distance. However, it is well known that numerical errors may accumulate due to repeated re-distance operations on a level set function. In order to prevent the straying of the zero level set from initial position even after many iterations, a mass constraint term proposed by Sussman and Fatemi (1999) is added to equation (7) as follows:

$$\begin{aligned} &\frac{\partial \phi}{\partial \tau} = L(\phi_0, \phi) + \lambda_{ij} f(\phi) \\ &\lambda_{ij} = -\int_{\Omega_{ij}} H'(\phi) L(\phi_0, \phi) \Big/ \int_{\Omega_{ij}} H'(\phi) f(\phi) \end{aligned} \tag{9}$$

where

$$\begin{aligned} &L(\phi_0, \phi) = sign(\phi_0)(1 - |\nabla \phi|) \\ &f(\phi) \equiv H'(\phi)|\nabla \phi| \end{aligned} \tag{10}$$

A more detailed description of the mass constraint term is given in Sussman and Fatemi (1999). The level-set method is incorporated into the dimensionless Reynolds-Averaged Navier-Stokes (RANS) equations for incompressible flow in general curvilinear coordinates (ξ^i, t) as follows:

$$U^i_{,i} = 0 \tag{11}$$

$$\frac{\partial U^i}{\partial t} + U^j U^i_{,j} + (\overline{u^i u^j})_{,j} = -\frac{\delta^i_3}{Fr^2} - \frac{g^{ij}}{\rho(\phi)} p_{,j} + \frac{\nu(\phi)}{Re} U^i_{,jk} \tag{12}$$

where U^i and u^i represent the mean and fluctuating velocity components, and g^{ij} is the conjugate metric tensor. t is time p is pressure, Fr is the Froude number, and $Re = U_o L/\nu$ is the Reynolds number based on a characteristic length L, a reference velocity U_o, and the kinematic viscosity ν. Equations (11) and (12) represent the continuity and mean momentum equations, respectively. The equations are written in tensor form with the subscripts, $,j$ and $,jk$, represent the

covariant derivatives. In the present study, the two-layer k-ε model of Chen and Patel (1988) is employed to provide closure for the Reynolds stress tensor $\overline{u^i u^j}$.

The present level-set RANS method has been used successfully in Chen and Yu (2006) for various two- and three-dimensional free surface flow applications involving violent free surface motions such as dam breaking and structure interactions, free jet problems, and greenwater on offshore structures. In the present study, the method is further generalized to provide accurate prediction of boundary layer flow and wall shear stresses along the levee surface.

Fig. 16 shows the geometry and overset (chimera) numerical grids for a two-dimensional levee cross section. The height of the levee is 5 m and the top width is 4 m. A 1/5 slope (i.e., 5 m / 25 m) was assumed for both sides of the levee. An initial water level of 6 m is specified with 1 m of overtopping on the levee top. The solution domain is 11 m high or 6 m above the top of the levee and the simulation was performed for both the water and air flows over the entire domain in a two-phase flow approach. In order to provide accurate resolution of the levee boundary layer, a 3 × 241 × 41 boundary-fitted grid was designed with fine grid spacing around the levee surface. The levee grid is embedded in a 3 × 301 × 85 rectangular grid with fine grid spacing near the bottom to resolve the basin boundary layer. A constant current of 3 m/s is specified on the left boundary of the rectangular solution domain.

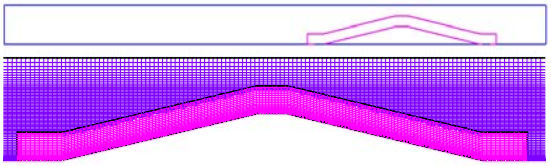

Figure 16 Geometry and partial view of numerical grid for a two-dimensional levee.

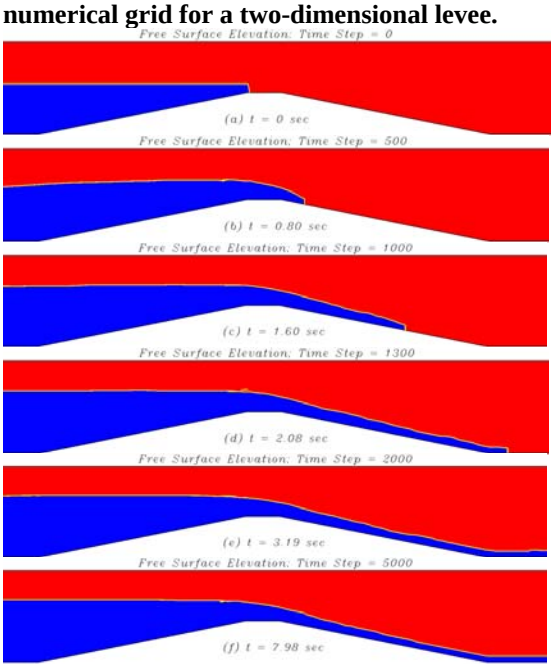

Figure 17 Figure 17 Free surface elevation contours at (a) t = 0, (b) t = 0.80 sec, (c) t = 1.60 sec, and (d) t = 2.08 sec, (e) t = 3.19 sec, and (f) t = 7.98 sec.

Fig. 17 shows the instantaneous free surface profiles at four different time instants. As noted earlier, the level-set functions were solved for the entire solution domain and the air-water interface is represented by the zero level-set function. At t = 0, the water is confined to the left hand side of the levee but the water level is 1 m above the level top. Due to the presence of strong current, the flow is pushed over the top of the levee and the water level upstream of the levee is rising during the initial stage of the simulation (Fig. 17b). On the downstream face of the levee, the water flow accelerates rapidly due to gravitational effect as seen in the velocity contour and vector plots shown in Fig. 18.

The water depth near the toe of the levee is considerably shallower than that on the levee top as the overtopping water flow velocity increases along the levee surface under the effects of gravity. The maximum velocity is close to 11.8 m/s around the toe of the downstream levee surface.

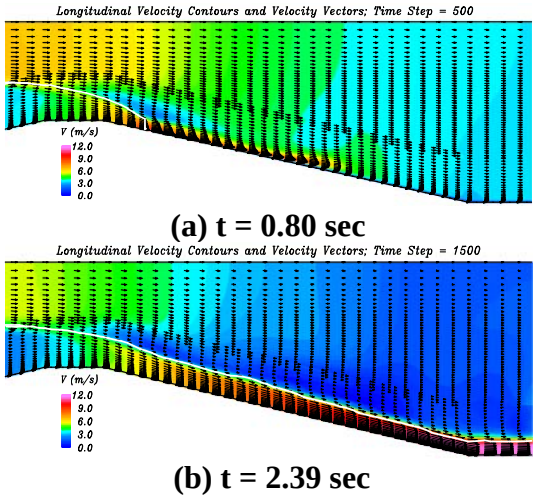

Figure 128 Longitudinal velocity contours and velocity vectors at (a) t = 0.80 sec, and (b) t = 2.39 sec.

CONCLUSIONS

Levees can resist overtopping. However the soil making up the levee must be able to resist the velocity and shear stress develop by the flow. The velocity and shear stress to be resisted can be obtained from 2D numerical simulations such as through the use of the program CHEN3D. The erosion function which links the velocity and shear stress to the erosion rate can be obtained with an apparatus such as the EFA.

Comparisons between the EFA measured erosion functions for samples taken from the New Orleans levees on one hand and the observed behavior of these levees helps in identifying what soils are most likely to resist erosion by overtopping.

Future work requires the evaluation of many miles of levees in the USA against erosion by overtopping. Levees are very long linear systems where a breach at one location defeats the whole system. A reasonable level of redundancy must be added to these systems of defense against the elements.

ACKNOWLEDGEMENTS

The authors wish to thank Raymond Seed and Robert Bea for giving them an opportunity to work with the Independent Levee Investigation Team (ILIT) sponsored by the National Science Foundation. The experience was unforgettable. We wish to thank Rune Storesund also with ILIT for his kindness, his organization skills, his attention to details, his tenacity, and his leadership. We enjoyed working with other members of ILIT: Diego Cobos-Rios, Carmen Cheung, Adda Athanasopoulos, all of whom showed some outstanding dedication to the task. Special thanks go to Paul Kemp for his great sense of cooperation. The authors also wish to thank all the students and professors who contributed to this study at Texas A&M University: Anand V Govindasamy, Keunyoung Rhee, Jennifer Nicks, Remon Abdelmalak, Ok-Youn Yu, Sam Youchmowitz**,** Ron Gardner, Tim Kramer, Namryong Her, Ming Han Li, Tony Provin. We also wish to thank Henk Verheij for reviewing the portion of the paper dealing with the Netherlands levees.

REFERENCES

1. ASTM D1587, American Society for Testing and Materials, Philadelphia, USA.
2. Bhandari, G., Sarkar, S. S., and Rao, G. V. (1998). Erosion control with geosynthetics, Geo-horizon: State of art in geosynthetic technology, A.A. Balkema, Rotterdam, Netherlands.
3. Briaud J.-L., (2006), "Erosion Tests on New Orleans Levee Samples", Internal Report, Civil Engineering, Texas A&M University, pp107.
4. Briaud J.-L., Chen H.-C., Kwak K., Wang J., Xu J., (2004), "The Sricos-FEA computer program for bridge scour", Proceedings of the Second Int. Conf. on Scour and Erosion, Singapore, Editor: Dr. Yee-Meng Chiew.
5. Briaud J.-L., Ting F., Chen H.C., Cao Y., Han S.-W., Kwak K., (2001), "Erosion Function Apparatus for Scour Rate Predictions". Journal of Geotechnical and Geoenvironmental Engineering, ASCE, Vol.127, No. 2, pp.105-113.
6. Briaud, J.-L., Ting, F., Chen, H.C., Gudavalli, S.R., Perugu, S., and Wei, G., (1999), "SRICOS: Prediction of Scour Rate in Cohesive Soils at Bridge Piers", ASCE Journal of Geotechnical Engineering, Vol.125, pp. 237-246.
7. Chen, H.C. (2002), "Numerical Simulation of Scour Around Complex Piers in Cohesive Soil," Proceedings of First International Conference on Scour of Foundations, pp. 14-33, November 17-20, College Station, Texas.
8. Chen, H.C. and Chen, M. (1998), "Chimera RANS Simulation of a Berthing DDG-51 Ship in Translational and Rotational Motions," Int. J. of Offshore and Polar Eng. Vol.8, No.3, pp. 182-191.
9. Chen, H.C. and Patel, V.C. (1988), "Near-Wall Turbulence Models for Complex Flows Including Separation," AIAA Journal, Vol. 26, No. 6, pp. 641-648.
10. Chen, H.C. and Yu, K. (2006), "Numerical Simulation of Wave Runup and Greenwater on Offshore Structures by a Level-Set RANS Method," 16th International Offshore and Polar Engineering Conference, May 28-June 2, San Francisco, California.
11. Chen, Y.H., Cotton, G.K., (1988), "Design of Roadside Channels with Flexible Linings," Federal Highway Administration, Hydraulic Engineering Circular No. 15.
12. CROW, (2000), "Standard RAW Regulations," The Netherlands.
13. Gerritsen, H. (2006), "The 1953 Dike Failures in the Netherlands, Geo-Strata, March-April 2006, p18-21, Geo-Institute of the American Society of Civil Engineers, Reston, Virginia, USA.
14. Moody L.F., (1944), "Friction Factors for Pipe Flow", Transaction of the American Society of Civil Engineers, Vol. 66, Reston, Virginia, USA.
15. Munson, B. R., Young, D. F., and Okiishi, T. H. (1990). Fundamentals of fluid mechanics. Wiley, New York.
16. Osher, S., and Sethian, J.A. (1988), "Fronts propagating with curvature-dependent speed: algorithms based on Hamilton-Jacobi formulations," Journal of Computational Physics, Vol. 79, No. 1, pp. 12-49.
17. Pilarczyk, K.W., (1998), "Dikes and revetments : design, maintenance and safety assessment", Balkema, Rotterdam, ISBN: 90-5410-455-4, 562 pp.

18. Pilarczyk, K.W., (1992), "Dutch Experience on Design of Dikes and Revetment," Coastal Engineering Practice '92, ASCE, pp. 794-813.
19. Seijffert, J.W., Verheij, H.J., (1998), "Grass covers and reinforcement measures," Chapter 14, Delft, The Netherlands.
20. Simm, J., (2005), COMRISK: Common Strategies to Reduce the Risk of Flooding in Coastal Lowlands, Sub-Project 4 Report, Performance of Risk Management Measures, The Netherlands.
21. Sussman, M. and Fatemi, E. (1999), "An Efficient, Interface-Preserving Level Set Redistancing Algorithm and Its Application to Interfacial Incompressible Fluid Flow," SIAM J. of Scientific Comput., Vol. 20, pp. 1165–1191.
22. Sussman, M., Smereka, P. and Osher, S. (1994), "A Level Set Approach for Computing Solutions to Incompressible Two-Phase Flow," Journal of Computational Physics, Vol. 114, pp. 146–159.
23. TAW (Technische Adviescommissie voor de Waterkeringen), (1998), "Technical Report on Water Retaining Structures," The Netherlands.
24. Verheij H. (2006), "Breach development in embankments of cohesive material", Delft Hydraulic, The Netherlands, http://www.wldelft.nl/rnd/intro/topic/breach-development/index.html
25. Verheij, H.J., (2002a), "Breaching in cohesive soils," WL|Delft Hydraulics, Research Report Q2959, Delft, The Netherlands.
26. Verheij, H.J., (2002b), "Time-dependent breach development in cohesive material," WL|Delft Hydraulics, Delft, The Netherlands.
27. Wu, T.H. (1995). Slope stabilization. In: R.P.C. Morgan, R.J. Rickson (Eds.). Slope Stabilization and Erosion Control: A Bioengineering Approach. E & FN Spon, London, pp. 221-264.